Microelectronic Engineering 88 (2011) 2158–2162

Contents lists available at ScienceDirect

Microelectronic Engineering

journal homepage: www.elsevier.com/locate/mee

Easy to adapt electron beam proximity effect correction parameter calibration based on visual inspection of a "Best Dose Sensor"

Nezih Unal [a,*], Martin D.B. Charlton [b], Yudong Wang [b], Ulrike Waizmann [c], Thomas Reindl [c], Ulrich Hofmann [a]

[a] GenISys GmbH, Eschenstraße 66, D-82024 Taufkirchen, Germany
[b] University Southampton, SECS, Southampton SO17 1BJ, UK
[c] Max-Planck-Institut für Festkörperforschung, Stuttgart D-70569, Germany

ARTICLE INFO

Article history:
Available online 15 February 2011

Keywords:
Electron beam lithography
Proximity effect
PEC parameter
Point spread function

ABSTRACT

The quality of e-beam proximity effect correction depends on the quality of the proximity effect model parameters, which are not accessible to direct measurement. Monte Carlo simulation is capable of determining the electron scattering coefficients, but does not include the process induced effects such as resist blur. Therefore, various experimental methods have been suggested (Stevensat et al. (1986) [1]; Rishton and Kern (1987) [2]; Hudek (2006) [3]). Most are either highly labor intensive due to a large required number of critical dimension measurements, or simple in the experimental evaluation, but limited in accuracy (Babin and Svintsov (1992) [4]), since resist effects interfere with the evaluation criterion.

This paper presents an easy to adapt experimental calibration method based on visual inspection of a "Best Dose Sensor", and its application to calibrate long- and mid-range effects.

© 2011 Elsevier B.V. All rights reserved.

1. Introduction

Electron beam lithography (EBL) is the most common technology for patterning nano-scale devices. Electron beams can be focused down to the 1 nm range, but the resolution is limited by extra effects such as electron scattering in the resist/substrate stack, resist material and development process effects. These effects cause imaging distortions with different influence ranges and strengths (proximity effects [5]) where the exposure of adjacent features interacts. As a consequence, the exposure result becomes dependent on the local layout density. All these proximity effects can be captured in a phenomenological point spread function PSF(r), that specifies the deposited energy of a point exposure at a distance r. The absorbed energy E in the resist now can be computed by convolving the applied dose $D(x,y)$ with that point spread function:

$$E(x,y) = D(x,y) \otimes \mathrm{PSF} := \int d^2r' D(r')\rho(r-r')$$

The point spread function can be approximated by a multi-Gaussian function:

$$\mathrm{PSF}(r) := (g_\alpha(r) + \nu_1^* g_{\gamma 1}(r) + \nu_2^* g_{\gamma 2}(r) + \eta^* g_\beta(r))/(1+\nu_1+\nu_2+\eta),$$

with g_σ being a normalized Gaussian of width σ.

As a matter of convention, α is used for short-range effects (shot size, beam blur, scattering in the resist and such), β and η are used for the long-range back-scatter contribution, and γ and ν are used for mid-range effects.

State-of-the-art proximity effect correction software (such as Layout BEAMER [6]) ensures that the absorbed energy at edges of features is uniform over the entire layout area, allowing correct development to occur simultaneously at the edges of all shapes. However the correction is only as good as the PSF used. Commercially available Monte Carlo software is capable of computing the electron scattering part of the PSF (for a given acceleration voltage and layer stack) with sufficient accuracy. The baseline for that simulation is electron – solid interactions – hence, resist material and process effects are not taken into account. In contrast, experimental methods for PSF calibration would include all effects, but methods published earlier [1–3] are either not accurate or require a large amount of exposure and accurate SEM measurement [4]. Since automated metrology tools (CD-SEM) are not typically available at nano-fabrication centers, required measurements are very time consuming and difficult to carry out.

2. Methods

This paper suggests a simplified practical methodology to rapidly calibrate proximity effect model parameters, based on simple experimental evaluation criterion that minimizes undesired resist

* Corresponding author.
E-mail address: unal@genisys-gmbh.com (N. Unal).

0167-9317/$ - see front matter © 2011 Elsevier B.V. All rights reserved.
doi:10.1016/j.mee.2011.02.066

effects (such as lateral development) in parallel. The methodology is capable of calibrating the proximity effect model parameters at various length scales, including electron scattering in the resist/substrate stack and/or resist material (such as β and η), as well as development process effects.

It consists of (i) intelligently designed calibration patterns, exposed at different exposure doses and (ii) a "best dose sensor" that allows the determination of correct dose for various layout densities by simple visual inspection. This sensor consists of a checkerboard pattern that exhibits a high detection sensitivity at the corners of a feature (see Fig. 1a), since the proximity effect in 2D (corners, line ends) is much stronger than the proximity effect in 1D (line width). The "best dose" can be identified by visually inspecting the corners of the squares, symmetry of squares with and without resist (see Fig. 1b). In order to increase the sensitivity of the sensor to dose changes, the exposures should be done at higher beam currents (e.g. several nA, since a larger beam blur results in larger effects, see Fig. 1c). The criterion for identifying the "optimum" dose depends on type, contrast and thickness of the resist – it can be as simple as checking if the corners of two butting squares are connected, or it may include related criterions such as exposed square/unexposed square symmetry (equivalent to them having the same size).

The sensor is positioned at various positions of calibration pattern. Identifying the "best dose" for various layout densities and length scales allows extraction of the proximity effect model parameters for the complete process, including the resist effects.

2.1. Base Dose and Eta (η) calibration

Proximity effect correction adjusts the exposure dose of localized areas of a pattern relative to an absolute Base Dose. The Base Dose in turn depends on the resist process (sensitivity, thickness, ...), the underlying material stack composition and accelerating voltage. Once properly calibrated, and used in conjunction with dose correction, the Base Dose becomes independent of pattern layout and underlying material stack.

The suggested pattern for the Base Dose calibration consists of a "Best Dose Sensor" positioned in the center of a large field, with width $>3 * \beta$, and a uniform pattern density of 50% (Fig. 2). The Base Dose is simply the optimal exposure dose for this "Best Dose Sensor" in the center. Please note the method is not limited to that 50% density – a different layout density would work as well, resulting in a different dose, and since the relationship between dose and layout density is known [7] ($D = (1 + \eta)/(1 + 2 * \text{density} * \eta)$), the result can also be used for the computation of η.

The sensor at the corner of this large field is used for η calibration. The relationship between dose and layout density given above can now be used to compute eta. For 50% layout density, the dose in the center will be 1. At the corner of the same pattern, the effective density is 12.5%, requiring a dose D12.5% for correct exposure. η can now be calculated by finding the optimal dose at the corner:

$$\eta = (D_{12.5\%} - 1)/(1 - 0.25 * D_{12.5\%})$$

Please note, that the Base Dose and η can be measured so simply, because the energy at the center and the corners of a large field are independent of β.

The concept for the determining β relies on the fact, that the Base Dose is the best dose for exposure at 50% layout density. Hence, a sensor sitting in the center of a circle with varying radii (Fig. 2b) will allow deriving β.

2.2. Short and mid-range calibration

The real value add of this methodology is its capability to determine the mid-range parameters caused by complex stack and process effects which are not covered by Monte Carlo simulation. The size of the squares and the overall sensor is varied in the range of expected mid-range effects (typically 50–500 nm), see Fig. 2c. The sensors are small (compared to the β range), and are exposed at varying exposure doses around Base Dose $* (1 + \eta)$ [7]. The SEM images of the different sized sensors exposed at best dose, over- and under-dose need to be analyzed to following criteria:

1. Evaluation of large sensors with uniform exposure (no distortions, good resolution):
   - The size of the squares at over- and under-dose and the rounding of corner allow the determination of the effective short-range blur α (the combination of beam size, forward scattering, and short-range process effects).
2. Evaluation of sensors around the resolution limit:
   - Getting to smaller size the checkerboard will start showing non-uniformity (the outer squares will be under-dose when the inner squares are over-dose). The influence range of the mid-range term γ is defined by the square size where the non-uniformity starts. The strength of the mid-range term v can be determined by evaluating the sensors at different doses.

The calibration is now a matter of matching the experimental results to simulation. Fig. 5 shows SEM images of different sensor sizes at different doses, in comparison to the best simulation fit for γ and v. The simulations were carried out by Layout BEAMER.

3. Experimental

The Base Dose and η calibration was validated at Southampton University using a JEOL JBX 9300 FS e-beam lithography

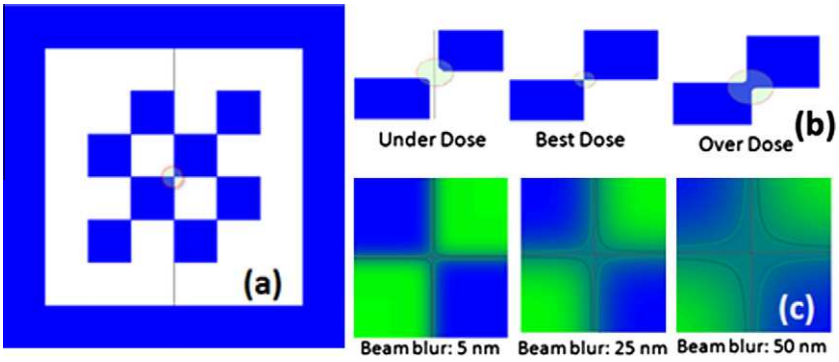

Fig. 1. The "Best Dose Sensor" using a checkerboard pattern (a) with a high sensitivity to dose changes at neighboring corners (b). Sensor sensitivity for ±10% dose variation depends on short-range blur (c).

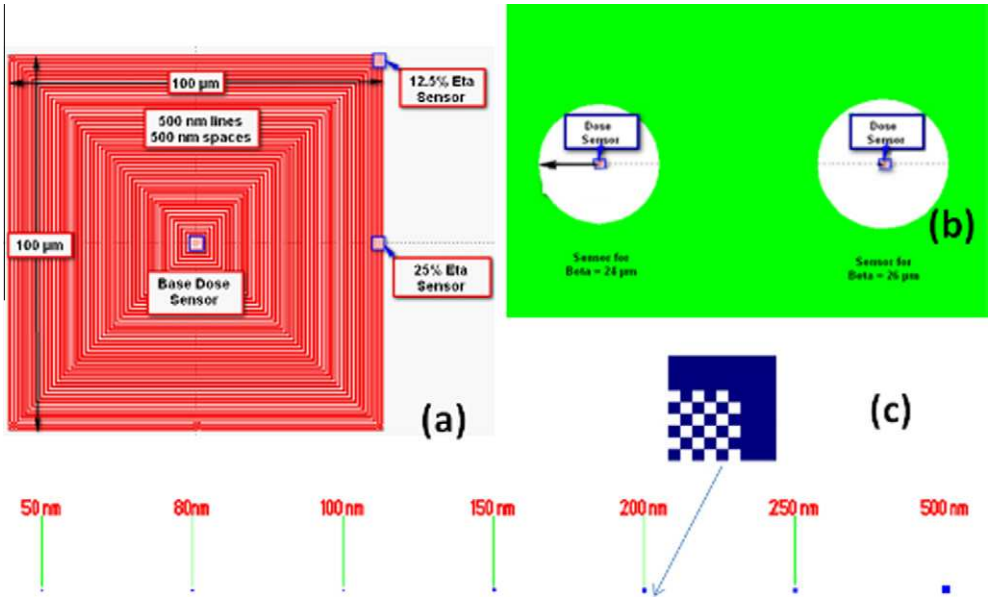

Fig. 2. Calibration pattern with Best Dose Sensor for Base Dose and Eta (a), for Beta (b) and for mid-range parameter (c).

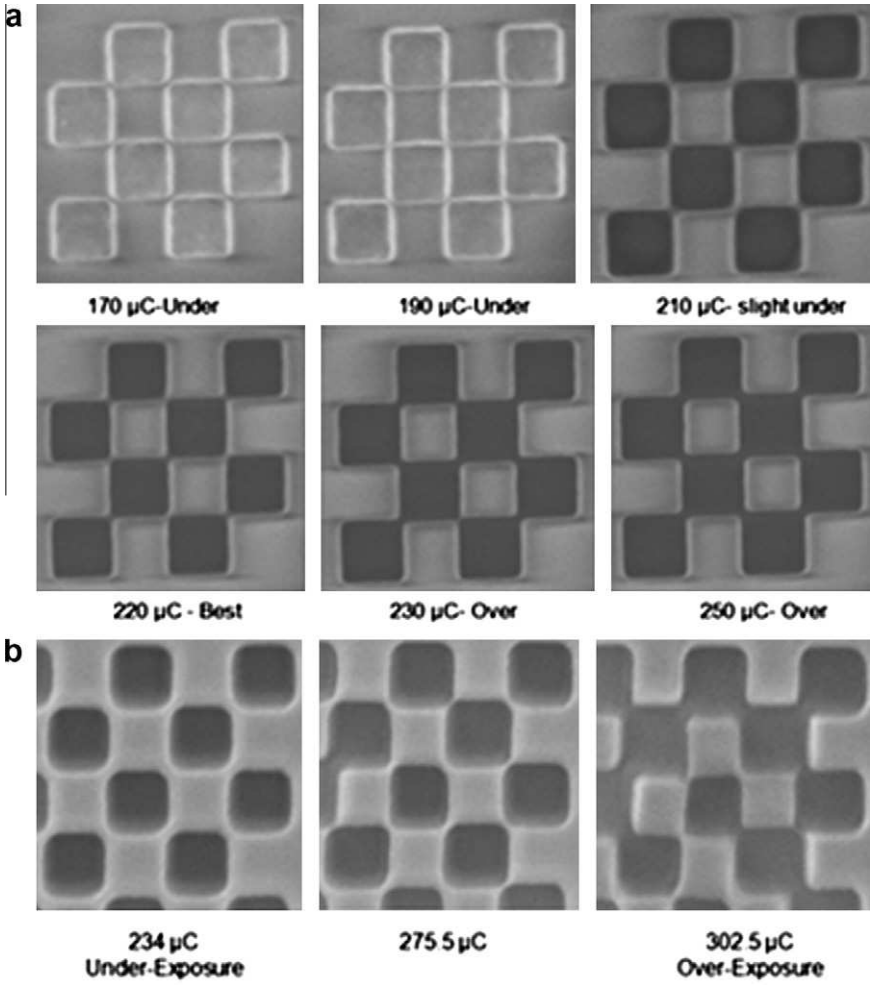

Fig. 3. One hundred kiloelectron volt exposure of Base Dose/Eta calibration pattern (50 μm size, 50% layout density) on silicon water with 400 nm ZEP 520A resist. (a) SEM picture of center sensor at different doses leading to the Best Dose of 220 μC/cm^2. (b) SEM picture for corner sensor at different doses leading to a Best Dose of 275 μC/cm^2.

system. Silicon wafers were spin coated with 400 nm thick ZEP520A positive tone resist, exposed at an acceleration voltage of 100 keV, 2 nA beam current, 6 nm exposure grid step, 100 μm final aperture size, and 6 nm spot size. Test substrates were developed using ZED-N50 for 90 s at 21 °C, then rinsed for 30 s in IPA.

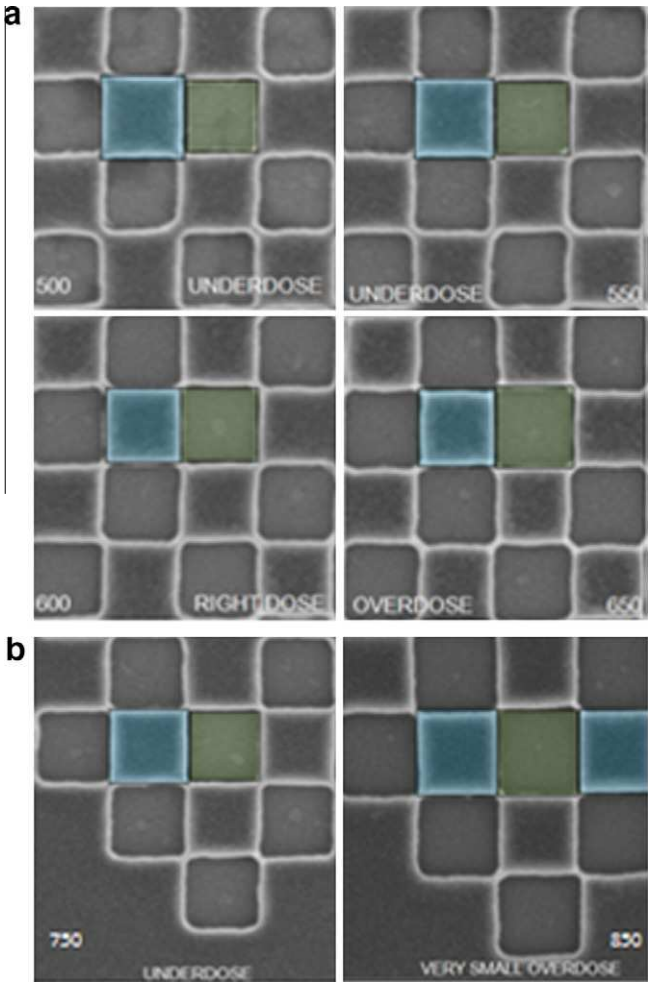

Fig. 4. One hundred kiloelectron volt exposure of Base Dose/Eta calibration pattern (100 μm size, 25% layout density) on GaAs wafer with 115 nm PMMA resist. (a) SEM picture of center sensor at different doses leading to the Best Dose of 600 μC/cm^2. (b) SEM picture for corner sensor at different doses leading to a Best Dose of 800 μC/cm^2.

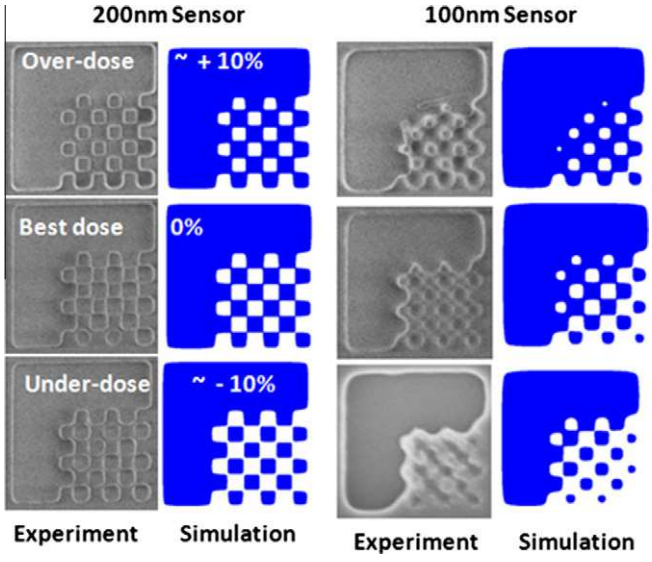

Fig. 5. Mid-range calibration pattern exposure results with 100 keV on Si wafer with 400 nm ZEP resist compared with simulation using short and mid-range setting of: α = 30 nm, γ = 150 nm, ν = 1.5.

In order to ensure full accuracy of the experimental results, imaging was performed using a JEOL JSM7500F SEM directly on the resist samples without application of any further metal coatings. In our experience, application of metal coating can cause shrinkage on the scale of 10 nm of small resist features due to resist heating effects. Similarly, to reduce e-beam induced damage and charging, imaging acceleration voltage was reduced to 0.9 kV, and a bias voltage applied to the substrate holder to prevent the sample from charging up (gentle beam mode). Probe current was kept to a minimum to reduce charging and increase resolution. In this mode it becomes possible to distinguish between fully cleared resist features, and structures with a very thin resist meniscus.

Fig. 3a shows SEM images of the central Base Dose sensor. The SEM images demonstrate that it is possible to determine the best exposure dose, by simple inspection of a small part of the pattern. In the case of underexposed conditions (170 and 190 μC/cm^2), a thin meniscus of undeveloped resist greatly reduces contrast in the exposed features, whereas correct or over exposed structures have very high contrast. In addition, examination of the quality of the corner bridge points of the patterned squares, and relative alignment of the inside bottom edge of the resist walls of neighboring features, enables the correct dose to be determined at 220 μC/cm^2. Unfortunately, the exposed calibration pattern was too small (extent of 50 μm) for the accelerating voltage of 100 keV ($<3 * \beta$), leading to a higher observed dose. It is known from literature that the back-scatter width for 100 kV exposures on Si is about 30 μm. That allows us to back-compute that the real Base Dose for a large enough pattern would have been 190 μC/cm^2. For the initial proof-of-concept that experimental flaw was tolerable, but for a precise measurement the large enough pattern would need to be used.

Fig. 3b shows SEM evaluation of the 12.5% η sensor in the corner at different exposure doses. This sensor shows the typical "bridge" for under-dose and the "gap" for over-dose between the square corners, leading to an optimal dose around 275 μC/cm^2, leading to an η of 0.66, in line with other techniques [8]. At optimal dose there is a small positive bias of exposed (removed) areas.

The same exposure condition has been used for exposing the mid-range calibration pattern with a small dose variation around Base Dose $*$ (1 + η) [7]. The 250 and 500 nm sensors did show uniform exposure over the checkerboard and no distortions. Using simulation to match the corner rounding and size difference between under- and over-dose the effective short-range blur α was determined to be 30 nm. The influence of the mid-range blur is visible at the 200 nm sensor (see Fig. 5) and is dominating at the 100 nm sensor, so that the checkerboard pattern cannot be resolved. Simulation with different mid-range influence ranges and strength matched best at γ = 150 nm and ν = 1.5.

The calibration of Base Dose and η has also been validated on GaAs substrates by experiments at the Max Planck Institute in Stuttgart using a JEOL JBX 6300 FS e-beam lithography system and 100 keV exposures. The beam current was 2 nA, giving a beam size of about 5 nm. The GaAs substrate was coated with 130 nm positive tone PMMA. From the SEM pictures (Fig. 4) the correct dose for the Base Dose Sensor (at the center) was determined to be about 600 μC/cm^2, and at the corner about 800 μC/cm^2. Taking the layout density in the center to be 25% and at the corner to be 6.25% we derive a Base Dose of 450 μC/cm^2 and η of 1.1.

4. Conclusion

An experimental proximity effect correction parameter calibration method was presented and verified on different substrates and resist processes. The method is based on visual inspection of SEM images of a "Best Dose Sensor" using a checkerboard design. The

evaluation criteria of the "best dose" requires some adaptation and process experience as the images are strongly depending on the resist process. The method has been validated for 100 keV exposure on silicon and on GaAs.

References

[1] L. Stevensat et al., Microelectron. Eng. 5 (1–4) (1986) 141–150.
[2] S.A. Rishton, D.P. Kern, J. Vac. Sci. Technol. B 5 (1) (1987) 135–141.
[3] P. Hudek, Microelectron. Eng. 83 (2006) 780–783.
[4] S.V. Babin, A.A. Svintsov, Microelectron. Eng. 17 (1992) 417–420.
[5] T.H.P. Chang et al., J. Vac. Sci. Technol. 12 (6) (1975) 1271–1275.
[6] Developed and distributed by GenISys GmbH. Available from: <www.genisys-gmbh.com/>.
[7] J. Pavkovich, J. Vac. Sci. Technol. B 4 (1) (1986).
[8] K. Keil et al., Microelectron. Eng. (2009), doi:10.1016/j.mee.2009.05.002.